# Assessment of the Performance of Image Fusion for the Mapping of Snow Using Euclidean Distance

***Pascal Sirguey[1], Sven Oltmer[2] & Renaud Mathieu[1]***

[1]Global Land Ice Measurements from Space (GLIMS) New Zealand Office
School of Surveying, University of Otago, PO Box 56, Dunedin, New Zealand
Phone: +64 3 479-7591 Fax: +64 3 479-7586
Email: sirpa271@student.otago.ac.nz
Email: renaud.mathieu@stonebow.otago.ac.nz

[2] Institute for Applied Photogrammetry and Geoinformatics (IAPG)
Department of Civil Engineering and Geoinformation
University of Applied Sciences Oldenburg/Ostfriesland/Wilhelmshaven
Ofener Strae 16-19, D-26121 Oldenburg, Germany
Email: sven.oltmer@stud.fh-oldenburg.de

**Presented at SIRC 2007 - The 19th Annual Colloquium of the Spatial Information Research Centre**
**University of Otago, Dunedin, New Zealand**
**December 6th-7th 2007**

## ABSTRACT

The assessment of the performance of multi-resolution image fusion, or image sharpening methods, is difficult. In the context of binary classification of snow targets in mountainous terrain, fusion methods were applied to help achieve more accurate mapping. To quantify objectively the gain of information that can be attributed to an increase in spatial resolution, we investigate the Mean Euclidean Distance (MED) between the snowline obtained from the classification, and a reference snowline (or a ground truth line), as a relevant indicator to measure both the discrepancy between datasets at different spatial resolutions, and the accuracy of the mapping process. First, a theoretical approach based on aggregating detailed reference images from the Advanced Spaceborne Thermal Emission and Reflection Radiometer (ASTER) showed that the MED has a linear relationship with the pixel size that makes it suitable to assess images of different resolutions. Secondly, we tested the MED to snow maps obtained 'with' or 'without' applying a fusion method to the MODerate Resolution Imaging Spectroradiometer (MODIS). We demonstrated that the MED identified a significant value added, in terms of mapping accuracy, which can be attributed to the fusion process. When the fusion method was applied to four different images, the MED overall decreased by more than 30%. Finally, such a 'feature based' quality indicator can also be interpreted as a statistical assessment of the planimetric accuracy of natural pattern outlines.

***Keywords and phrases:*** Image fusion, Image sharpening, Metric, Snow, Snowline, Remote sensing, Euclidean distance, MODIS

## 1 INTRODUCTION

In the context of remote sensing, image fusion consists of merging images from different sources, which hold information of a different nature, to create a synthesized image that retains the most desirable characteristics of each source (Pohl & Genderen 1998, Zhang 2004, Amolins, Zhang & Dare 2007). For instance, many optical sensors (e.g. SPOT, IKONOS, QUICKBIRD) routinely acquire simultaneously one panchromatic image (PAN), covering a wide part of the electromagnetic spectrum, and one multispectral image (MS), including several bands at a coarser spatial resolution (i.e. pixel size). Other sensors, such as the MODerate Resolution Imaging Spectroradiometer (MODIS) or the Advanced Spaceborne Thermal Emission and Reflection Radiometer (ASTER), do not hold a PAN band, but numerous spectral bands with different spatial resolutions. In this context, multispectral fusion methods usually aim to merge the rich spatial content of a high spatial resolution image (HR, e.g. PAN band) with the rich spectral content of a low spatial resolution image (LR, e.g. MS bands) (Garguet-Duport, Girel,

Chassery & Pautou 1996, Ranchin, Aiazzi, Alparone, Baronti & Wald 2003, González-Audicana, Saleta, Catalán & García 2004, Tu, Huang, Hung & Chang 2004, Zhang & Kang 2006). Fusion is becoming popular in various field due to its ability to improve the detection and extraction of ground targets (Nichol & Wong 2005, Lasaponara & Masini 2005, Malpica 2007), or the spatial resolution of post-classified products (Pasqualini, Pergent-Martini, Pergent, Agreil, Skoufas, Sourbes & Tsirika 2005, Jin & Davis 2005, Sirguey, Mathieu, Arnaud, Khan & Chanussot 2008). In most cases the assessment of the quality of the fusion or the gain of information obtained through the fusion remains challenging.

In order to improve the details of snow maps in mountainous terrain, Sirguey et al. (2008) proposed to fuse the rich spatial content of the 250-m resolution MODIS HR bands into the 500-m resolution MODIS LR bands that are spectrally required to map the snow. The method was validated by comparing MODIS-derived snow maps, obtained 'without' or 'with' the fusion process, with reference maps obtained simultaneously from 15-m resolution ASTER imagery. A visual analysis eventually concluded an improvement in the ability to map snow with the fused images. However, this subjective method does not provide a quantitative measure that would objectively score the improvement. Therefore both integrated and pixel-based metrics were investigated. Nevertheless, comparing images of different resolution is difficult and raises the issue of multi-scale analysis (Woodcock & Strahler 1987, Lam & Quattrochi 1992). Not all metrics are adequate to assess the gain of information generated by an increase of spatial resolution (Sirguey et al. 2008). Pixel-based metrics should be established with maps having the same spatial resolution, in order to be comparable. Consequently, the 250-m resolution maps of subpixel snow fraction were aggregated at 500 m prior to computing the pixel-based metrics. This approach demonstrated that the fusion significantly add information, but it cannot truly account for the fact that the snow was mapped at an improved resolution of 250-m pixel size. A metric capable of operating independently from the pixel size is therefore desirable.

In this article, we propose to investigate the potential of the Mean Euclidean Distance (MED) between the seasonal snowlines extracted from the MODIS-derived snow maps (either at 500-m or 250-m spatial resolution, i.e. 'without' or 'with' fusion) and the reference ASTER snowline, as a relevant metric to assess the gain that the fusion provides in terms of snow cover delineation capability. We based our reasoning on the fact that edges and contours are essential in the understanding of natural scenes, and therefore the better the contours are depicted, the higher the quality of the image (Zhai, Zhang, Yang & Xu 2005). In the first part of this article, we briefly review the strategies and issues raised by the quality assessment of fused products. In the second part, we present the data and the methodology implemented to assess the performance of the MED as a metric. Finally, we present and discuss the sensitivity of this metric to various parameters, and its efficiency when applied to the MODIS-derived snow maps obtained 'without' or 'with' implementing the fusion method.

## 2 BACKGROUND ON QUALITY ASSESSMENT OF MULTISPECTRAL FUSION

Image fusion algorithms often create radiometric distortions and/or artefacts (Wald, Ranchin & Mangolini 1997, Du, Vachon & van der Sanden 2003, Tu et al. 2004, González-Audicana, Otazu, Fors & Alvarez-Mozos 2006). Therefore, it is required to estimate the quality of the fusion process, in order to assess its performance and robustness, as well as the usability of the fused product. The validation of image fusion is a difficult task, which usually rely on the investigation of both subjective and objective methods (Aiazzi, Alparone, Argenti & Baronti 1999, Gao, Wang & Li 2005, Shi, Zhu, Tian & Nichol 2005, Laporterie-Déjean, de Boissezon, Flouzat & Lefèvre-Fonollosa 2005, Alparone, Wald, Chanussot, Thomas, Gamba & Bruce 2007, Petrovic 2007).

### 2.1 Qualitative analysis

Subjective methods are based on the visual analysis of the fused image. They aim to provide a judgment (e.g. an opinion score) on the quality of the fused product according to a prior set of criteria, defined with regard to the needs of the users (Petrovic 2007, Laporterie-Déjean et al. 2005). However, because it involves the subjective human visual perception, such qualitative assessment is inevitably biased by the observer's experiences and appreciation (Toet & Franken 2003, Chen & Varshney 2007). Visual analysis is a powerful tool to assess improvement, because of its ability to capture spatial details as the resolution of the image increases, but it fails to account accurately for the preservation of the radiometry in the image. Therefore its consistency in terms of scientific value with regard to the original data is questionable.

### 2.2 Quantitavive analysis

Numerous researches report on the design of metrics to assess objectively the quality of fused images (Wald et al. 1997, Ranchin & Wald 2000, Wald 2000, Xydeas & Petrovic 2000, Wang & Bovik 2002, Alparone, Baronti, Garzelli & Nencini 2004). The metrics are usually based on and/or derived from standard descriptive statistics

(e.g. bias or difference of means, Root Mean Square Error RMSE, coefficient of correlation CC, coefficient of determination $R^2$, standard deviation $\sigma$). They aim to quantify the discrepancy between the fused image and a reference, to measure both the gain of information generated by an increase of spatial resolution, and its spectral integrity with regard to the original spectral content. Since no reference image is obviously available at the finer resolution (resolution of the fused image) a popular protocol consists in the assessment of the method at a coarser resolution (Wald et al. 1997). HR and LR images are degraded relatively to their resolution so that the pixel size of the degraded HR matches the original LR. The fusion process is computed with the degraded images. The original LR can then be used as a genuine reference in the process of validation. In case of a successful assessment, the method is assumed to perform similarly at the finer scale.

## 2.3 Assessment through the validation of end-products

The validation protocols described previously are limited to the investigation of the fused image itself. They aim to score the quality of the image that is obtained with the fusion, with regard to the theoretical image that would have been acquired if the sensor had the desired spatial resolution. Sometimes, however, the images obtained from the fusion are to be post-processed (e.g. semantic classification of ground targets, or retrieval of physical parameter), to create a specific end-product with an increased spatial resolution. In this case, the relevancy and performance of the fusion can eventually be measured in terms of the quality of the post-processed product, rather than the quality of the fused images only. Such validation strategy aims to prove that there is a significant improvement in the end-product, if the fusion is processed prior to post-processing the image. It is this strategy that we use in the present article. Indeed, we aim to estimate the accuracy, in terms of position, of the seasonal snowline, which can be extracted from MODIS-derived snow maps obtained 'with' or 'without' using the multispectral fusion.

# 3 DATA

Four pairs of simultaneous MODIS/ASTER acquisitions selected at different seasons and including various conditions of snow cover were selected in the Aoraki/Mount Cook region, New Zealand (see dates in Tab. 1).

## 3.1 MODIS-derived subpixel snow fraction

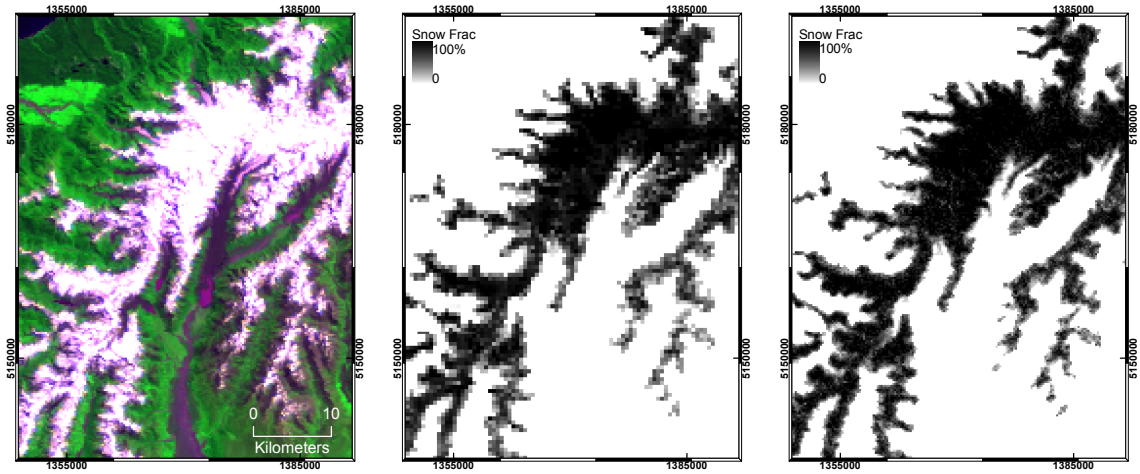


(a) (b) (c)

Figure 1: *Example of subpixel snow map created from MODIS imagery (Mt Cook Area, South Island of New Zealand, 31 December 2002 22:35 GMT) : (a) False colour RGB composite with MODIS bands 1, 2 (250 m) and 3 (fused to 250 m). (b) Subpixel snow fraction computed from MODIS bands at 500 m. (c) Subpixel snow fraction computed from MODIS bands fused at 250 m.*

The four MODIS images were processed according to the methods described in more details in Sirguey et al. (2008). These include the following steps: georectification of MODIS-Terra L1B swath data products (MOD02QKM, MOD02HKM, MOD021KM, MOD03), wavelet-based fusion between MODIS 250-m bands and

MODIS 500-m bands, and implementation of a topographic and atmospheric correction model as described by Richter (1998). Finally, a constrained spectral unmixing technique was applied (Keshava 2003), either to the seven original 500-m bands or the seven 250-m bands obtained 'with' the fusion, to produce maps of subpixel snow fractions. Figure 1 shows an example of a MODIS-derived map of subpixel snow fraction. Figure 1(b) and Figure 1(c) show the snow maps obtained 'without' and 'with' the fusion, at 500 m and 250 m, respectively. They illustrate the improvement that can be achieved when implementing the fusion.

### 3.2 Reference snow cover from ASTER

The four corresponding ASTER images were orthorectified and matched to the MODIS images. An example showing a simultaneous ASTER/MODIS pair is given in Figure 2(a). The spatial resolution of ASTER (15 m) images compared to the 250 m and 500 m resolution of MODIS images provides a ratio of 277 and 1111 ASTER pixels, respectively, for each MODIS pixel. We therefore hypothesized that a binary classification of snow from ASTER would provide accurate ground truth of the snow cover distribution. The snow was binary classified using the Normalized Difference Snow Index (NDSI) that takes advantage of the contrast between the high reflectance of snow in the green part of the visible spectrum (ASTER Band 1 at 560 nm) and its low reflectance in the short wave infrared (ASTER Band 4 at 1640 nm) (Equation 1) (Crane & Anderson 1984).

$$NDSI = \frac{\rho^*_{560nm} - \rho^*_{1640nm}}{\rho^*_{560nm} + \rho^*_{1640nm}} \tag{1}$$

where $\rho^*$ is the apparent reflectance measured at the top of atmosphere by ASTER. A custom threshold of 0.7 was chosen to binary classified the snow according to the NDSI value, based on visual analysis of the image and the investigation of the histogram of the NDSI image. Such a relatively high threshold insures that pixels are fully covered with snow. From the binary classification, it is possible to extract the reference seasonal snowline, which stands for the boundary between the group of pixels classified as 'snow' or 'no snow'.

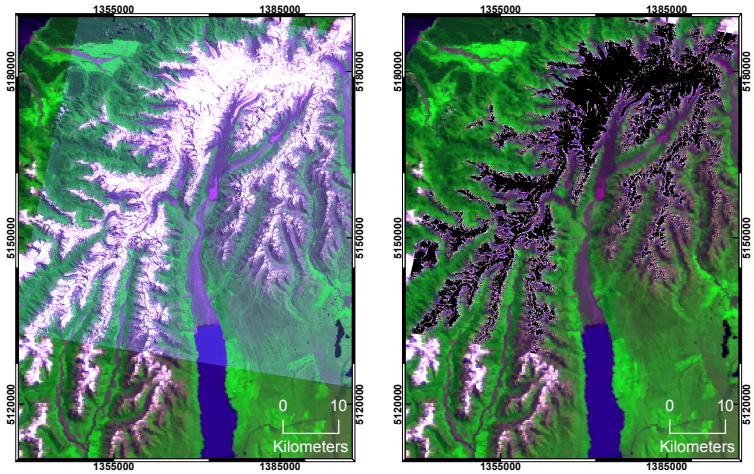


(a) (b)

Figure 2: *Example of simultaneous ASTER and MODIS imagery (Mt Cook Area, South Island of New Zealand, 31 December 2002 22:35 GMT) : (a) False colour RGB composite from ASTER bands 2, 3, 1 (15 m) overlaid onto a false colour RGB composite from MODIS bands 1, 2 (250 m) and 3 (fused to 250 m). The difference of spatial resolution is clearly visible when zooming in the pdf version of this document. (b) Binary snow map from ASTER used as reference and overlaid onto the MODIS RGB composite (pixels classified as snow are drawn in black; pixels without snow are transparent).*

## 4 METHODOLOGY

### 4.1 Object-based metrics

The quality assessment of classified end-products or maps is usually based on a 'per-pixel' approach. It refers to the assessment of agreement and confusions that occur between the classified image and the ground or a more

detailed reference image. Recently, object-based indicators have also been developed to provide a more comprehensive assessment of the quality of geo-spatial objects (Zhan, Molenaar, Tempfli & Shi 2005). In an object-based environment, Zhan et al. (2005) suggested that new measures accounting for the correct classification, size and position of the objects, can be used along with 'per-pixel' measures to assess quality. Li, He, Bu, Wen, Chang, Hu & Li (2005) also investigated the behaviour of numerous simple and sophisticated geo-spatial metrics to several parameters, such as number of classes, map extent, resolution, class proportion and aggregation. Li et al. (2005) concluded that metrics can be sensitive to pattern scenarios, and not all metrics are adequate to compare landscape maps with different resolutions. From a quantitative point of view, sophisticated metrics based on multi-scale analysis have been designed to assess the quality of contour and edges in the image (Zhai et al. 2005). Because geometrical features are essential in the understanding of natural scenes, such investigation may be appropriate to assess the added value of fusion to end-products. In the context of designing a metric $d$ that would score a set $x$ according to a reference, it is desirable to state what is expected from the measure:

1. The metric should provide a positive score: $d(x) \geq 0$.
2. If the set $x$ matches the reference, then $d(x) = 0$ and reciprocally.
3. If the set $x$ matches the reference better than the set $y$, then $d(x) \leq d(y)$ and reciprocally.
4. Metrics computed on images of different spatial resolution can be compared.
5. The magnitude of change of the metric must match the magnitude of change in spatial resolution.

Nevertheless, one must keep in mind that, in mapping sciences, the development of a metric to assess the quality of geo-spatial objects can sometimes raise issues related to the fractal theory (Goodchild 1980, Lam & Quattrochi 1992). For instance, due to the fractal nature of natural boundaries such as coastline, watershed or landscape natural pattern (Goodchild & Mark 1987), a metric based on the perimeter of natural objects can appear irrelevant, because it would depend on its measurement gauge (e.g. the spatial resolution in the context of remote sensing). In other words, the perimeter of an object can have a non-finite or fractal dimension, that makes its use inconsistent to the design of a metric (Bendjoudi 2002).

## 4.2 Calculation of Euclidean Distance

We based our approach on the seasonal snowline as representative object. It is assumed that mapping the snow cover with a higher spatial resolution will provide a snowline that better depicts the reality. The Mean Euclidean Distance (MED), calculated in a two-dimensional space, between the line extracted from the classifier or 'test line', and the 'reference snowline' (extracted from 15-m ASTER imagery), can be seen as a quantitative indicator of this match. For any given point $P$ of the 'test snowline', its Euclidean distance $D(P)$ to the 'reference snowline' $S$, as shown on Figure 3, can be formulated as the norm of the smallest vector that can be drawn between $P$ and $S$ (Figure 3):

$$\forall P \in I, D(P) = \min_{Q \in S} \left\| \overrightarrow{PQ} \right\| \tag{2}$$

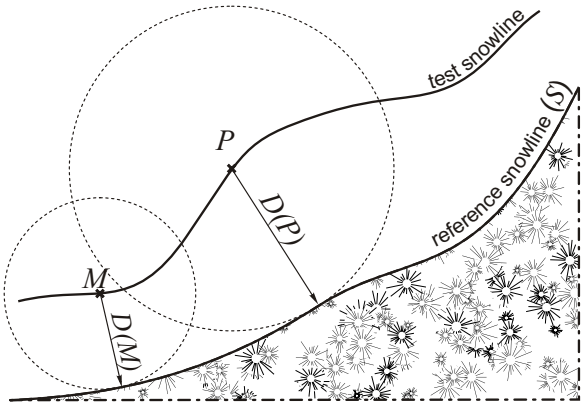


Figure 3: *Minimum Euclidean distance $D(P)$ between a point $P$ on the 'test snowline' and the 'reference snowline' $S$.*

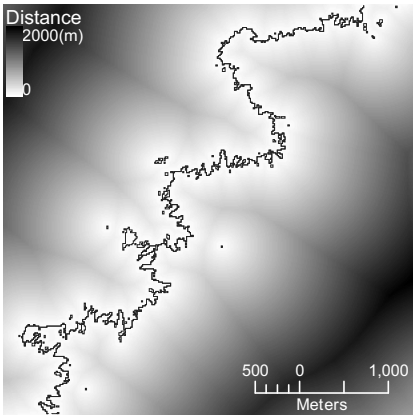


Figure 4: *Example of Euclidean distance raster image created at 12.5 m pixel size and computed from the ASTER (15 m) reference snowline.*

Although there is, of course, uncertainty in the measurement of Euclidean distance between any points of a test snowline to the reference snowline, it is possible to determine lower and upper bounds at all resolutions (i.e. the MED will always range between 0 and the maximum length of the image diagonal). The dimension of such measure is therefore non-fractal. From the computational point of view, the Euclidean distance cannot be easily computed for all points of a continuous line, but it can be estimated according to a set of samples. A raster image which contains the measured distance from every cell to its closest point of the 'reference snowline' can be created. The pixel size of this 'distance raster' must be smaller or equal than the pixel size at which the 'reference snowline' was mapped. An example of 'distance raster' is shown in Figure 4. The cells of this raster, that are intersected by the snowline to be tested, account for a representative distribution of Euclidean Distance, from which standard descriptive statistics can be inferred (e.g. MED, standard deviation $\sigma$).

## 4.3 Investigation strategy

### 4.3.1 Theoretical behaviour of MED using ASTER reference data

To assess the relevancy of the MED as a metric capable of scoring binary classification independently of the spatial resolution, we investigated its theoretical behaviour when used with reference material only, simulated for various pixel size. From the original ASTER binary snow map, it is possible to derivate maps of subpixel snow fraction that will be used as reference materials to investigate the sensitivity of the MED to pixel size. The four original ASTER binary snow maps were first resampled at 12.5m, then aggregated to 50 m, 125 m, 250 m, 500 m and 1000 m to create a reference dataset of multi-resolution maps, all originating from the same groundtruth. Figure 5(a) and (b) shows an example of the 250-m and 500-m aggregations of Figure 2(b).

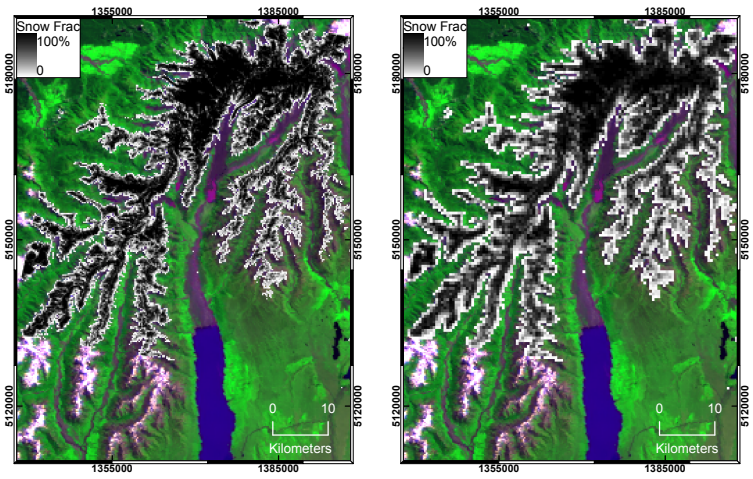


Figure 5: *Example of aggregation of the ASTER binary snow map at various spatial resolution (Mt Cook Area, South Island of New Zealand, 31 December 2002 22:35 GMT): (a) Reference subpixel snow fraction map at 250 m resolution aggregated from the 15-m resolution binary classification (pixels without snow are transparent). (b) Reference subpixel snow fraction map at 500 m resolution aggregated from the 15-m resolution binary classification (pixels without snow are transparent).*

The computation of Euclidean distances requires binary classes (e.g. 'snow' or 'no snow'). In our case, the reference snow maps, aggregated from the original ASTER 15-m binary classification, provide subpixel snow fraction for various pixel size. A threshold must be defined to achieve a crisp representation of this continuous quantity, and thus indicate if the pixel should be accounted for 'snow' or 'no snow' at a given resolution. A reasonable assumption could be to set a pixels as 'snow', if it is covered with more than 50% of snow. By using this threshold, Figure 6 illustrates how the match between the snowlines extracted from various spatial resolutions and the original 15-m 'reference snowline' degrades as the pixel size increases. Nevertheless, the sensitivity of the MED to the threshold of snow cover must be investigated, in order to determine the most appropriate threshold to depict accurately the snowline. For all dates, the 250-m resolution maps of subpixel snow fraction were binary classified, with increasing thresholds of subpixel snow fraction, in order to assess this sensitivity.

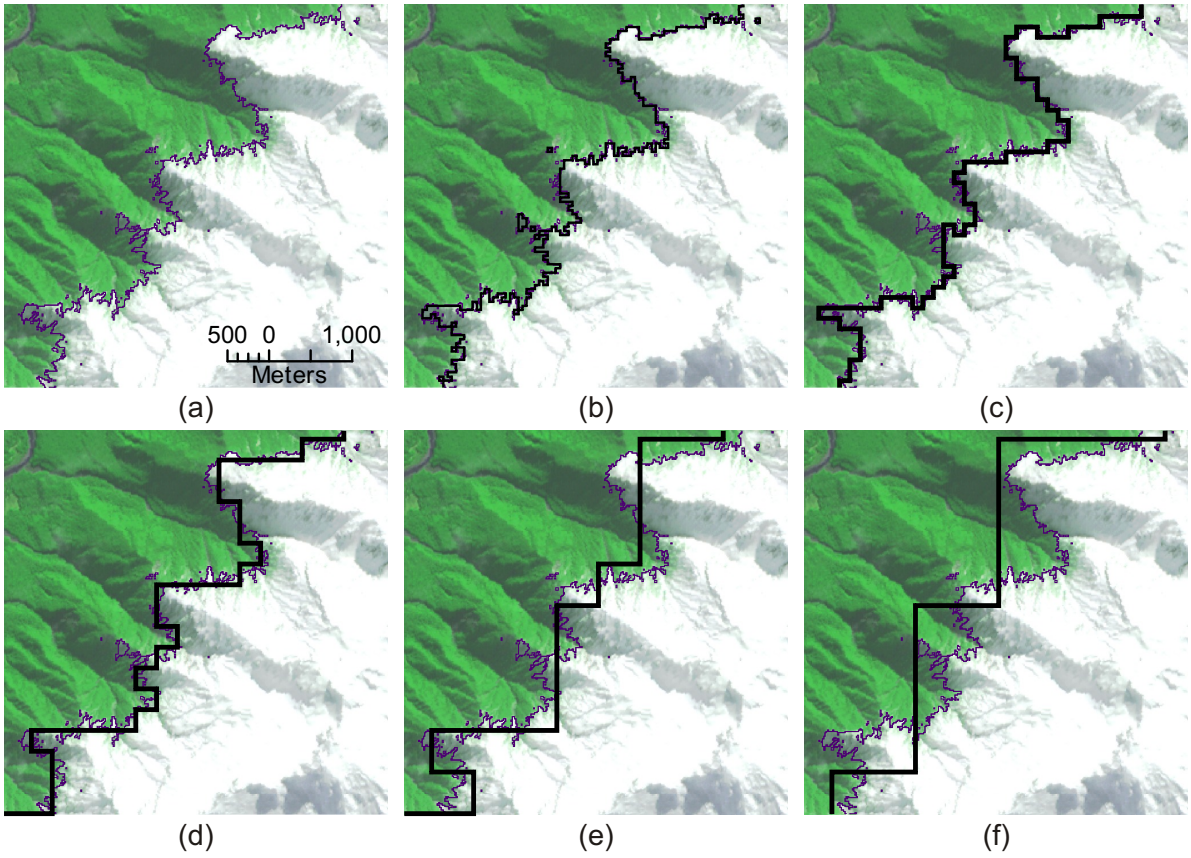


Figure 6: *Example of seasonal snowlines extracted from an ASTER image at different spatial resolution. (a) 15-m resolution snowline used as reference extracted from the binary snow classification of the ASTER image (ground truth); (b), (c), (d), (e) and (f) show the snowlines extracted after aggregation of the ASTER binary snow map at 50 m, 125 m, 250 m, 500 m and 1000 m spatial resolution, respectively.*

By definition, aggregated maps of ASTER subpixel snow fraction integrate, in one pixel, all the information in term of distribution that can be found in the original 15-m resolution binary map. This information accounts for numerous small snow patches that can be found, usually, nearby the main snow-covered entity. Snow patches, that are smaller than half the area of an aggregated pixel, either contribute positively to map the pixel as 'snow', or are excluded from the aggregated map. In this case however, they are problematic, because they act as small 'islands' where the 'distance raster' has small values (Figure 4). These 'islands' of small distances can bias the estimation of the snowline MED. Indeed, as the pixel size increases, the aggregated snow map tends to map bigger objects. Keeping all small features therefore leads to an increasing probability of intercepting small distances. However, a significant part of these small values artificially comes from patches that are not accounted in the main object. Similar bias can occur for small 'no snow' patches, inside the snow cover, nearby the main snowline. Such patches are illustrated in Figure 7. To address this issue, a 'cleaning' strategy was implemented, dependent on the resolution for which the MED will be computed. For a given resolution, all patches smaller than half the area of the pixel are removed prior to computing the 'distance raster'. Later in the paper, 'cleaning' and 'no cleaning' refer to values of MED that are computed with and without implementing this strategy, respectively.

#### 4.3.2 Application of MED to real fused and non fused MODIS snow maps

Once the theoretical behaviour of the MED was defined using ASTER derived reference material, the MED metric was applied to the MODIS 'real case'. The snowlines were extracted from both the 250-m and 500-m resolution maps of subpixel snow fraction, obtained 'with' and 'without' the fusion method, respectively. The MEDs to the ASTER 15-m reference snowline were computed to quantify the ability of the fusion to achieve a better delineation of seasonal snowline with MODIS-derived snow maps.

In order to insure that the supposed additional information truly originates from the implementation of the fusion method, we compared the previous results with the MEDs of snowlines that were extracted after the re-

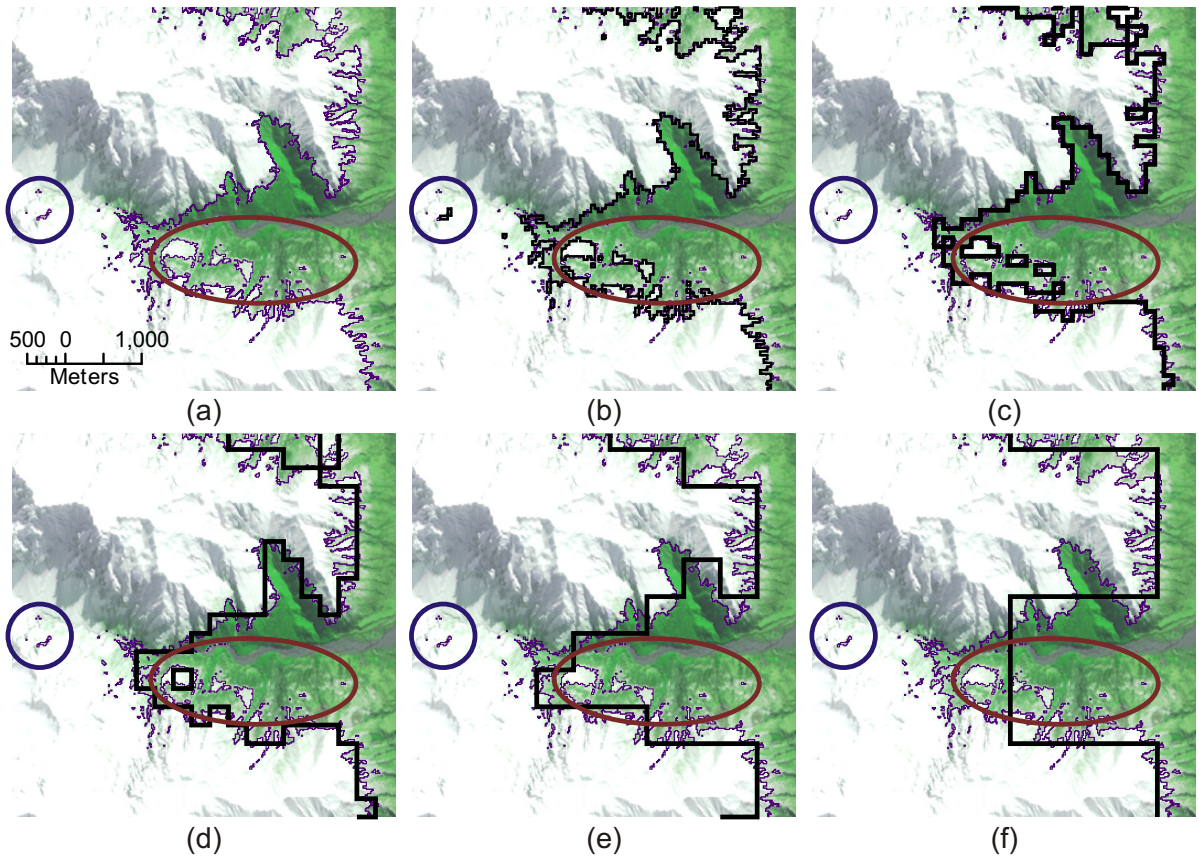


Figure 7: *Illustration of the influence of small patches on the determination of snowlines at various spatial resolutions. (a) 15-m resolution snowline used as reference extracted from the binary snow classification of the ASTER image (ground truth); (b), (c), (d), (e) and (f) show the snowlines extracted after aggregation of the ASTER binary snow map at 50 m, 125 m, 250 m, 500 m and 1000 m spatial resolution, respectively. The ellipses shows snow patches of different sizes, the circles shows "snow voids" within the main snow entity that can alter the value of Euclidean distance.*

sampling of the 500-m subpixel snow fraction at 250 m resolution using a simple bicubic interpolator.

# 5 RESULTS AND DISCUSSION

## 5.1 Metric behaviour

An investigation of the behaviour of the metric to different parameters is essential to confirm the relevancy of this approach. Initially, we used only the set of reference snowlines extracted at 15 m from ASTER, along with maps of subpixel snow fraction that were derived by aggregating the binary map at various pixel sizes.

Figure 8 shows the behaviour of the MED of the resulting snowline as a function of the threshold used to segment the map of subpixel snow fraction. It clearly confirms that, as expected, the shortest average distance is achieved for a snowline created from pixels having more than 50% snow cover. Based on this result, all MED will be computed after classification of the subpixel snow fraction using the 50% threshold.

Because they are all derived from the same 15-m reference, the ASTER-derived maps of subpixel snow fraction, successively aggregated at 50 m, 125 m, 250 m, 500 m and 1000 m, provide the reference dataset to estimate the sensitivity of the MED to pixel size. Figure 9 shows that the MED significantly increases with the pixel size, both when cleaning or keeping the smallest snow patches. It confirms our assumption that the snowline is generally closer to the reference as the resolution increases, meaning a better match. When computing the MED without the 'cleaning' strategy, it is interesting to note that the relationship between the MED and the pixel size is not linear. In this case, the dispersion of the MED according to the different dates (see error bars on Figure 9), is significant, suggesting that the metric may be sensitive to the area covered by snow, and eventually the number of snow patches. However, when applying the 'cleaning' strategy, the MED becomes significantly correlated to

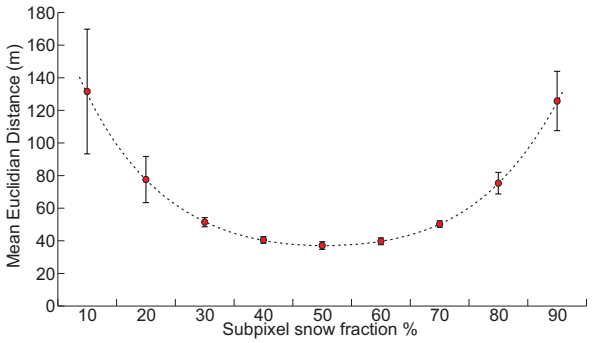


Figure 8: *Sensitivity of the Mean Euclidean Distance (MED) to the subpixel snow fraction used to binary classifies the snow cover map. For all dates, the ASTER-derived 250-m resolution maps of subpixel snow fraction were binary classified, with increasing thresholds of subpixel snow fraction. The error bars indicate the standard deviation of the MED for to the four images.*

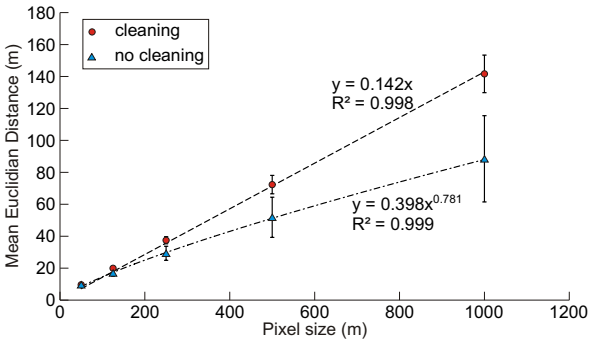


Figure 9: *Sensitivity of the Mean Euclidean Distance (MED) to the aggregation of the binary ASTER-derived snow cover map. The error bars indicate the standard deviation of the MED for to the four images.*

the pixel size. The dispersion of the MED between the different dates is also greatly reduced. This confirms the significant impact of the small patches in such a multi-scale analysis. Further, when applying the 'cleaning' strategy the MED consistently drops by 50% when pixel size is reduced by a factor of two. This matches the magnitude of theoretical change that is desirable in the framework of designing an indicator that assesses the quality of a feature as the resolution increases. This validation can be interpreted as a calibration of the metric. It sets a milestone in terms of what can be expected as an improvement in a real case, for instance by fusing 250-m MODIS bands with 500-m MODIS bands. Simultaneously, the distribution of Euclidean Distances for all samples along the whole test snowline also provides a statistical estimation of 'how far' it lay from the reality. The mean of the distribution, along with its standard deviation, provides a quantitative insight in terms of the planimetric accuracy of the snowline position.

## 5.2 Application to MODIS-derived snow map

Table 1: Mean and standard deviation $\sigma$ of the Euclidean Distance calculated between the snowline obtained from MODIS-derived snow maps, and the reference snowline extracted from ASTER at 15 m. 'Type' '250 m' refers to the snowline extracted from the MODIS-derived snow map at 250 m resolution obtained with fusion. 'Type' '500 m' refers to the snowline extracted from the MODIS-derived snow map at 500 m resolution obtained without fusion. 'Type' "interp. 250 m" refers to the snowline extracted after bicubic interpolation at 250 m of the 500-m resolution MODIS-derived snow map.

| Date | Type | Without cleaning | | With cleaning | |
|---|---|---|---|---|---|
| | | MED (m) | $\sigma$ (m) | MED (m) | $\sigma$ (m) |
| 31/12/2002 | **250 m** | **31** | 36 | **56** | 58 |
| | interp. 250 m | 38 | 43 | 71 | 69 |
| | 500 m | 44 | 52 | 90 | 87 |
| 29/01/2002 | **250 m** | **56** | 64 | **80** | 95 |
| | interp. 250 m | 64 | 65 | 85 | 82 |
| | 500 m | 76 | 80 | 109 | 107 |
| 16/05/2006 | **250 m** | **80** | 123 | **110** | 155 |
| | interp. 250 m | 113 | 146 | 182 | 245 |
| | 500 m | 102 | 124 | 187 | 241 |
| 11/09/2000 | **250 m** | **76** | 127 | **119** | 263 |
| | interp. 250 m | 89 | 112 | 130 | 210 |
| | 500 m | 103 | 118 | 151 | 209 |

The results of applying this method to the MODIS dataset are shown in Table 1. For all dates, whether

applying the cleaning strategy or not, the MED values inferred from the 250-m resolution maps using the fusion, are significantly smaller than those derived from the 500-m resolution map. The MED dropped about 26% on average (min 22%, max 30%), when not cleaning the smallest snow patches, and about 32% on average (min 21%, max 41%) when using the cleaning strategy. This magnitude of improvement must be compared to the 50% improvement that is expected in an ideal case when reducing the pixel size by a factor of two. It suggests that, as expected, the fusion does not achieve what would be obtained if we had real 250-m MODIS-derived snow map. Nevertheless, the planimetric accuracy of the snowline position has increased of 60% in comparison with the ASTER reference snowline.

The MED of the snowline obtained from the interpolated map improved 8% and 15% without and with the cleaning strategy, respectively. This improvement was expected since the interpolation process was likely to move the snowline towards the reference due to the correlation of the subpixel snow fraction in space. Nevertheless, the range of improvement is still half what was achieved with the fusion. This comparison suggests that the fusion adds significantly more information, with regard to the accuracy of snow distribution, than a simple interpolation.

The MED is higher for the two winter images than the summer one, suggesting that the classification is more accurate in summer. The presence of stronger shadow effects, along with a larger snow extent in winter images, is expected to increase the noise in the process of retrieving the subpixel snow fraction. The lower quality for the winter images is consistent with what was previously observed by Sirguey et al. (2008).

## 6 CONCLUSION

The Mean Euclidean Distance (MED) has been investigated as a relevant metric to objectively assess the improvement of the snow mapping process, following an increase of the spatial resolution of MODIS bands using image fusion. In this study, we assumed that in the case of a binary segmentation of the image, the quality of the classification can be assessed by an estimation of how well the boundary between the two classes 'snow' and 'no snow' matches the reality.

The sensitivity of the MED to the spatial resolution was investigated using reference images obtained from ASTER and proved the MED to be suitable to objectively quantify such match or discrepancy. The metric also revealed objectively that in the case of a continuous classification of subpixel snow fraction, the 50% snow covered limit is the optimum threshold to depict the snowline. Our investigation of a real case involving fusion applied to MODIS imagery, showed that: (1) The MED of the 250-m resolution snow map, obtained with the fusion, was significantly lower than the MED of the 500-m snow map. The 32% decrease of the MED means the fusion provided 64% of the accuracy improvement that could ideally be achieved, if we had real 250-m resolution bands; and (2) although a significant improvement in terms of MED can be achieved by a simple interpolation of the 500-m resolution snow map to 250 m resolution, the interpolation clearly failed to depict as much information as the fusion. We suggest that this metric can be useful to assess the performance of image fusion, along with other protocols, such as visual interpretation and pixel-based image quality assessment, but with the advantage of being comparable at all resolutions.

In addition, the investigation of the distribution of Euclidean Distance, between a class boundary and a corresponding reference, also provides a comprehensive and useful insight with regard to the planimetric accuracy of class boundaries. Although, in this study, the MED indicator has been designed for binary classification of snow, it can be suitable to assess the quality of various natural pattern outlines. In the case of more classes, the use of this indicator in a more sophisticated strategy can be investigated, to both assess the position of boundaries and the correct classification of the objects on each side of the boundary. However, it is obviously important to address the issue raised by small patches that can bias the metric, and modify its linear behaviour according to the resolution.

## References


Aiazzi, B., Alparone, L., Argenti, F. & Baronti, S. (1999). "Wavelet and pyramid techniques for multisensor data fusion: a performance comparison varying with scale ratios" In S. B. Serpico (ed.), *Proceedings of the SPIE Image Signal Process. For Remote Sensing V*. Vol. 3871 SPIE SPIE. pp. 251–262.

Alparone, L., Baronti, S., Garzelli, A. & Nencini, F. (2004). "A global quality measurement of pan-sharpened multispectral imagery" *IEEE Geoscience and Remote Sensing Letters*. **1**(4): 313–317.

Alparone, L., Wald, L., Chanussot, J., Thomas, Gamba, P. & Bruce, L. M. (2007). "Comparison of pansharpening algorithms: outcome of the 2006 GRS-S data fusion contest" *IEEE Transactions on Geoscience and Remote Sensing*. **45**(10): 3012–3021.

Amolins, K., Zhang, Y. & Dare, P. (2007). "Wavelet based image fusion techniques – An introduction, review and comparison" *Journal of Photogrammetry and Remote Sensing*. **62**(4): 249–263.

Bendjoudi, H. (2002). "The gravelius compactness coefficient: critical analysis of a shape index for drainage basins" *Hydrological Sciences Journal*. **47**(6): 921–930.

Chen, H. & Varshney, P. K. (2007). "A human perception inspired quality metric for image fusion based on regional information" *Information Fusion*. **8**(2): 193–207.

Crane, R. G. & Anderson, M. R. (1984). "Satellite discrimination of snow / cloud surfaces" *International Journal of Remote Sensing*. **5**: 213–223.

Du, Y., Vachon, P. W. & van der Sanden, J. J. (2003). "Satellite image fusion with multiscale wavelet analysis for marine applications: preserving spatial information and minimizing artifacts (PSIMA)" *Canadian Journal of Remote Sensing*. **29**(1): 14–23.

Gao, X., Wang, T. & Li, J. (2005). "A content-based image quality metric" *Lecture Notes in Computer Science*. **3642**: 231–240. to get.

Garguet-Duport, B., Girel, J., Chassery, J.-M. & Pautou, G. (1996). "The use of multi-resolution analysis and wavelet transform for merging SPOT panchromatic and multispectral imagery data" *Photogrammetric Engineering and Remote Sensing*. **62**(9): 1057–1066.

González-Audicana, M., Otazu, X., Fors, O. & Alvarez-Mozos, J. (2006). "A low computational-cost method to fuse IKONOS images using the spectral response function of its sensors" *IEEE Transactions on Geoscience and Remote Sensing*. **44**(6): 1683–1691.

González-Audicana, M., Saleta, J. L., Catalán, R. G. & García, R. (2004). "Fusion of multispectral and panchromatic images using improved IHS and PCA mergers based on wavelet decomposition" *IEEE Transactions on Geoscience and Remote Sensing*. **42**(6): 1291–1299.

Goodchild, M. (1980). "Fractals and the accuracy of geographical measures" *Mathematical Geology*. **12**(2): 85–98.

Goodchild, M. F. & Mark, D. M. (1987). "The fractal nature of geographic phenomena" *Annals of Association of American Geographers*. **77**(2): 265–278.

Jin, X. Y. & Davis, C. H. (2005). "Automated building extraction from high-resolution satellite imagery in urban areas using structural, contextual, and spectral information" *EURASIP Journal of Applied Signal Processing*. **2005**(14): 2196–2206.

Keshava, N. (2003). "A survey of spectral unmixing algorithms" *Lincoln Laboratory Journal*. **14**(1): 55–78.

Lam, N. S.-N. & Quattrochi, D. A. (1992). "On the issues of scale, resolution, and fractal analysis in the mapping sciences" *Professional Geographer*. **44**(1): 88–98.

Laporterie-Déjean, F., de Boissezon, H., Flouzat, G. & Lefèvre-Fonollosa, M.-J. (2005). "Thematic and statistical evaluations of five panchromatic/multispectral fusion methods on simulated PLEIADES-HR images" *Information Fusion*. **6**(3): 193–212.

Lasaponara, R. & Masini, N. (2005). "QuickBird-based analysis for the spatial characterization of archaeological sites: case study of the Monte Serico medieval village" *Geophysical Research Letter*. **32**(12): L12313.

Li, X., He, H. S., Bu, R., Wen, Q., Chang, Y., Hu, Y. & Li, Y. (2005). "The adequacy of different landscape metrics for various landscape patterns" *Pattern Recognition*. **38**(12): 2626–2638.

Malpica, J. A. (2007). "Hue adjustment to IHS pan-sharpened IKONOS imagery for vegetation enhancement" *IEEE Geoscience and Remote Sensing Letters*. **4**(1): 27–31.

Nichol, J. & Wong, M. S. (2005). "Satellite remote sensing for detailed landslide inventories using change detection and image fusion" *International Journal of Remote Sensing*. **26**(9): 1913–1926.

Pasqualini, V., Pergent-Martini, C., Pergent, G., Agreil, M., Skoufas, G., Sourbes, L. & Tsirika, A. (2005). "Use of SPOT 5 for mapping seagrasses: An application to Posidonia oceanica" *Remote Sensing of Environment*. **94**(1): 39–45.

Petrovic, V. (2007). "Subjective tests for image fusion evaluation and objective metric validation" *Information Fusion*. **8**(2): 208–216.

Pohl, C. & Genderen, J. L. V. (1998). "Multisensor image fusion in remote sensing: concepts, methods and applications" *International Journal of Remote Sensing*. **19**(5): 823–854.

Ranchin, T., Aiazzi, B., Alparone, L., Baronti, S. & Wald, L. (2003). "Image fusion–the ARSIS concept and some successful implementation schemes" *Journal of Photogrammetry and Remote Sensing*. **58**: 4–18.

Ranchin, T. & Wald, L. (2000). "Fusion of high spatial and spectral resolution images : the ARSIS concept and its implementation" *Photogrammetric Engineering and Remote Sensing*. **66**(1): 49–61.

Richter, R. (1998). "Correction of satellite imagery over mountainous terrain" *Applied Optics*. **37**(18): 4004–4015.

Shi, W., Zhu, C., Tian, Y. & Nichol, J. (2005). "Wavelet-based image fusion and quality assessment" *International Journal of Applied Earth Observation and Geoinformation*. **6**: 241–251.

Sirguey, P., Mathieu, R., Arnaud, Y., Khan, M. M. & Chanussot, J. (2008). "Improving MODIS spatial resolution for snow mapping using wavelet fusion and ARSIS concept" *IEEE Geoscience and Remote Sensing Letters*. **5**(1): doi:10.1109/LGRS.2007.908884. In Press.

Toet, A. & Franken, E. M. (2003). "Perceptual evaluation of different image fusion schemes" *Displays*. **24**(1): 25–37.

Tu, T.-M., Huang, P. S., Hung, C.-L. & Chang, C.-P. (2004). "A fast Intensity–Hue–Saturation fusion technique with spectral adjustment for IKONOS imagery" *IEEE Geoscience and Remote Sensing Letters*. **1**(4): 309–312.

Wald, L. (2000). "Quality of high resolution synthesized images: is there a simple criterion?" *Proceedings of the International Conference on Fusion of Earth Data*. SEE Gréca Sophia Antipolis, France pp. 99–105.

Wald, L., Ranchin, T. & Mangolini, M. (1997). "Fusion of satellite images of different spatial resolution: assessing the quality of resulting images" *Photogrammetric Engineering and Remote Sensing*. **63**(6): 691–699.

Wang, Z. & Bovik, A. C. (2002). "A universal image quality index" *IEEE Signal Processing Letters*. **9**(3): 81–84.

Woodcock, C. E. & Strahler, A. H. (1987). "The factor of scale in remote sensing" *Remote Sensing of Environment*. **21**(3): 311–332.

Xydeas, C. S. & Petrovic, V. (2000). "Objective image fusion performance measure" *Electronics Letters*. **36**(4): 308–309.

Zhai, G., Zhang, W., Yang, X. & Xu, Y. (2005). "Image quality assessment metrics based on multi-scale edge presentation" *Proceedings of the IEEE Workshop on Signal Processing Systems Design and Implementation*. IEEE IEEE. pp. 331–336.

Zhan, Q., Molenaar, M., Tempfli, K. & Shi, W. (2005). "Quality assessment for geo-spatial objects derived from remotely sensed data" *International Journal of Remote Sensing*. **26**(14): 2953–2974.

Zhang, W. J. & Kang, J. Y. (2006). "QuickBird panchromatic and multi-spectral image fusion using wavelet packet transform" *Intelligent Control and Automation*. **344**: 976–981.

Zhang, Y. (2004). "Understanding image fusion" *Photogrammetric Engineering and Remote Sensing*. **70**(6): 657–661.